



# OPEN Prenatal bisphenol A exposure causes sperm quality and functional defects via Leydig cell impairment and meiosis arrest in mice offspring

Wendi Zhang<sup>1,4</sup>, Juan Liu<sup>1,2,4</sup>, Yanhua Wang<sup>3</sup>, Jiahui Wang<sup>1,2</sup>, Peng Zhu<sup>1</sup>, Wenting Wang<sup>1,2</sup>, Zhan Song<sup>1</sup>, Jun Li<sup>1</sup>, Dan Song<sup>1</sup>, Yanwei Wang<sup>1✉</sup> & Xin Liu<sup>1,2✉</sup>

Bisphenol A (BPA), widely used in plastic production, acts as an environmental endocrine disruptor which is harmful to male reproductive health. However, the specific mechanisms through which prenatal BPA exposure disrupts spermatogenesis in offspring, particularly in terms of Leydig cell dysfunction and meiotic progression, remain poorly understood. To address this gap, we constructed a mouse model with BPA lowest Observed Adverse Effect Level (LOAEL: 50 mg/kg bw/day) exposure from embryonic day (ED) 0.5 to 18.5. Our results demonstrated that prenatal BPA exposure significantly decreased serum testosterone levels, testis weight, sperm count, motility parameters, and acrosomal integrity. Furthermore, it arrested the meiotic transition from zygotene to pachytene spermatocytes, leading to reduced sperm fertility characterized by reduced sperm-egg binding capacity and abnormal early embryonic cleavage in the male offspring. Importantly, prenatal BPA exposure significantly reduced the expression of PCNA (a marker of germ cell proliferation), SYCP3 (a meiosis regulator), and Vimentin (a blood-testis barrier component), collectively indicating impaired spermatogenesis in offspring testes. Additionally, prenatal BPA exposure dramatically reduced Leydig cell numbers and increased apoptosis, marked by BAX/BCL2 up-regulation, which mechanistically explains the observed testosterone reduction. In vitro experiments corroborated these effects: BPA exposure concentration-dependently inhibited Leydig cell proliferation, induced G0/G1 phase arrest, and downregulated testosterone synthesis molecules (Hsd3b1, Hsd17b3, Star, Cyp11a1, Cyp17a1). Quantitative proteomics identified 234 differentially expressed proteins (97 downregulated, 137 upregulated) in BPA-exposed Leydig cells. Bioinformatics analysis revealed that down-regulated proteins were mainly related to steroid hormone receptor activity, estrogen response element binding, and centrosome duplication processes, while the up-regulated proteins were mainly involved in oxygen binding and ROS metabolic process. Conclusively, prenatal BPA exposure impaired offspring male fertility via multi-faceted mechanisms: sperm quality defects, steroidogenic disruption, and meiotic arrest. This study advances the understanding of BPA transgenerational reproductive toxicity and underscores the need to mitigate prenatal exposure risks.

**Keywords** Bisphenol A, Offspring toxicity, Meiosis, Sperm defects, Male subfertility

Bisphenol A (BPA), designated by IUPAC as 4-[2-(4-hydroxyphenyl)propane-2-yl]phenol, acts as an environmental endocrine disruptor and is unfortunately still one of the most mass-produced chemicals worldwide. BPA can permeate into water, soil, animals, plants, and other systems. It has been detected in human saliva, blood, plasma, amniotic fluid, placental tissue, breast milk, urine, follicular fluid, and adipose tissue. Many studies have indicated that BPA can cause abnormalities in health, including male and female infertility, many kinds of malignant tumors, neuroendocrine issues, thyroid problems, metabolism disorder and obesity,

<sup>1</sup>Central Laboratory, Yantai Yuhuangding Hospital, Yantai 264000, China. <sup>2</sup>Shandong Stem Cell Engineering Technology Research Center, Yantai Yuhuangding Hospital, Yantai 264000, China. <sup>3</sup>Department of Medical Records Room, Weifang People's Hospital, Weifang 261000, China. <sup>4</sup>Wendi Zhang and Juan Liu contributed equally to this work. ✉email: fortunexinw@163.com; dkgha@163.com

and cardiovascular endocrine issues<sup>1–3</sup>. BPA is structurally similar to 17 $\beta$ -estradiol (E2) and can bind to both  $\alpha$  (ER $\alpha$ ) and  $\beta$  estrogen receptors (ER $\beta$ )<sup>4</sup>. It can also bind directly to androgen receptors (AR), possibly acting as an anti-androgen and blocking endogenous androgen action. BPA also can alter endocrine functions related to testosterone levels, reduce semen quality, and lead to delayed conception time<sup>5</sup>. Continuous exposure to BPA reduces sperm count and motility, increases DNA damage and malfunction, and ultimately leads to poor sperm quality and reduced fertility. Eventually, it leads to poor sperm quality and reduced fertility<sup>6,7</sup>. Compared to adults, fetuses and babies have immature metabolic systems, so they are at greater risk of exposure and accumulation of BPA. BPA has been detected at concentrations ranging from 0.14 to 9.2 ng/g in fetal cord blood, 1.3 to 50.5 ng/g in fetal liver, and 0.36 to 5.62 ng/g in amniotic fluid. It has been indicated that the fetus may be exposed to BPA by parental uptake<sup>8–10</sup>.

The fetus, infants, and children may have increased sensitivity to environmental stressors such as EDCs due to their rapid development. The risk of EDC exposure is further increased due to developmental-specific behavioral, anatomical, and physiological reasons<sup>11,12</sup>. The effects of exposure during organ development can be directly measured during exposure and persist throughout the life activities of animals<sup>13</sup>. However, some studies have shown that the effects of BPA exposure during organ development may not be detectable immediately but become apparent in subsequent adulthood. There is evidence that the effects of BPA on tissues is mediated by epigenetic DNA changes<sup>14</sup>. BPA exposure alters core histone proteins, which could ultimately lead to male infertility<sup>15</sup>, and may also result in a significant decrease of H3K9me2 activity in the testes, leading to the loss of spermatogonia and meiotic germ cell<sup>16</sup>. Different durations of BPA exposure in utero can affect testicular DNA methylation and ultimately reproductive function, disrupt fetal gonadal programming through dysregulated fatty acid metabolism in offspring testes, and cause differences in anogenital distance, nipple retention, onset of puberty, spermatogonial stage, and testicular morphology in offspring<sup>17,18</sup>. Although some studies have indicated that BPA exposure impaired testicular function, few studies investigated changes in sperm quality and function induced by prenatal BPA exposure.

In this study, we constructed a mouse model with BPA exposure (LOAEL: 50 mg/kg bw/day) from embryonic day (ED) 0.5–18.5. We determined their reproductive phenotypes and examined the altered critical biological processes of spermatogenesis and sperm functions in offspring exposed to BPA prenatally. Prenatal BPA exposure impaired male offspring fertility by affecting sperm quality and function, disturbing steroidogenesis and the proteome of Leydig cells and arresting zygotene-pachytene transition during meiotic spermatogenesis. This study provides essential information for further investigating the molecular mechanisms involved in prenatal BPA exposure and its effects on male reproduction.

## Materials and methods

### Animals and treatment

All animal experiments complied with the ARRIVE guidelines and were approved by the Animal Ethics Committee of Yantai Yuhuangding Hospital (approval No. 2023-006). All procedures for animal care and use were carried out following the guidelines for the care and use of laboratory animals in accordance with the US NIH Guide for the Care and Use of Laboratory Animals (no. 8023, revised in 1996). All efforts were made to minimize the number of animals used and to reduce suffering during the experiment.

Adult ICR mice (6–7 weeks old, 24–27 g, Beijing Vital River Laboratory Animal Technology Co., Ltd., Beijing, China) were housed under a 12 h/12 h light/dark cycle at constant room temperature (23  $\pm$  1  $^{\circ}$ C) with free access to food and water. Two female mice were placed overnight with 1 male mouse for mating. Detection of a vaginal plug the next morning was designated embryonic developmental day (ED) 0.5. Mice were randomly assigned to two groups: a control group ( $n$  = 15) receiving corn oil and a BPA-treated group ( $n$  = 15) administered 50 mg/kg/day BPA via oral gavage from ED 0.5 to ED 18.5 (Fig. 1). At the end of experiment, the mice were deeply anesthetized with 20 ml/kg BW 1.25% Avertin (2,2,2-tribromoethanol, Nanjing AiBei Biotechnology Co. Ltd., China) and were euthanized by cervical dislocation.

### Sperm parameters and serum testosterone in male offspring mice

On postnatal day (PND) 70, sperm from the caudal epididymis were collected for analysis of parameters and function. The body and testis weights of male offspring mice were measured. The epididymides were rapidly cut into small pieces and incubated at 35  $^{\circ}$ C in normal saline for 5 min, and the released spermatozoa were collected for analyzing sperm parameters using the Computer Aided Semen Analysis (CASA) System (Medealab<sup>™</sup>, Erlangen, Germany). Blood was collected, and serum testosterone were measured according to the instruction of Testosterone EIA Kit (Cayman, CAY-582751–96 S, SUA). Daily sperm production (DSP) was estimated using a previous described method<sup>19</sup>.

### Sperm acrosome integrity

Cauda epididymal sperm from five control and five prenatal BPA-exposed mice were collected and smeared. The sections were stained with FITC-PSA (L0770, Sigma, St. Louis, MO, USA) at 4  $^{\circ}$ C for 1 h and the nuclei were stained with 4',6-diamidino-2-phenylindol (DAPI), then washed with phosphate buffered saline (PBS). At least 200 spermatozoa were evaluated per slide under an Axio Observer Z1/7 fluorescence microscope.

### Male fertility assay with in vitro fertilization (IVF) experiment

As previously described<sup>20</sup>, approximately 10<sup>4</sup> sperm were used to incubate with oocytes for 6 h. The average number of sperm bound to oocytes was calculated. The percentage of two-cell embryos relative to the number of prokaryotic oocytes was considered the embryonic development rate, whereas the percentage of eight-cell embryos relative to the number of two-cell embryos was considered the eight-cell formation rate.

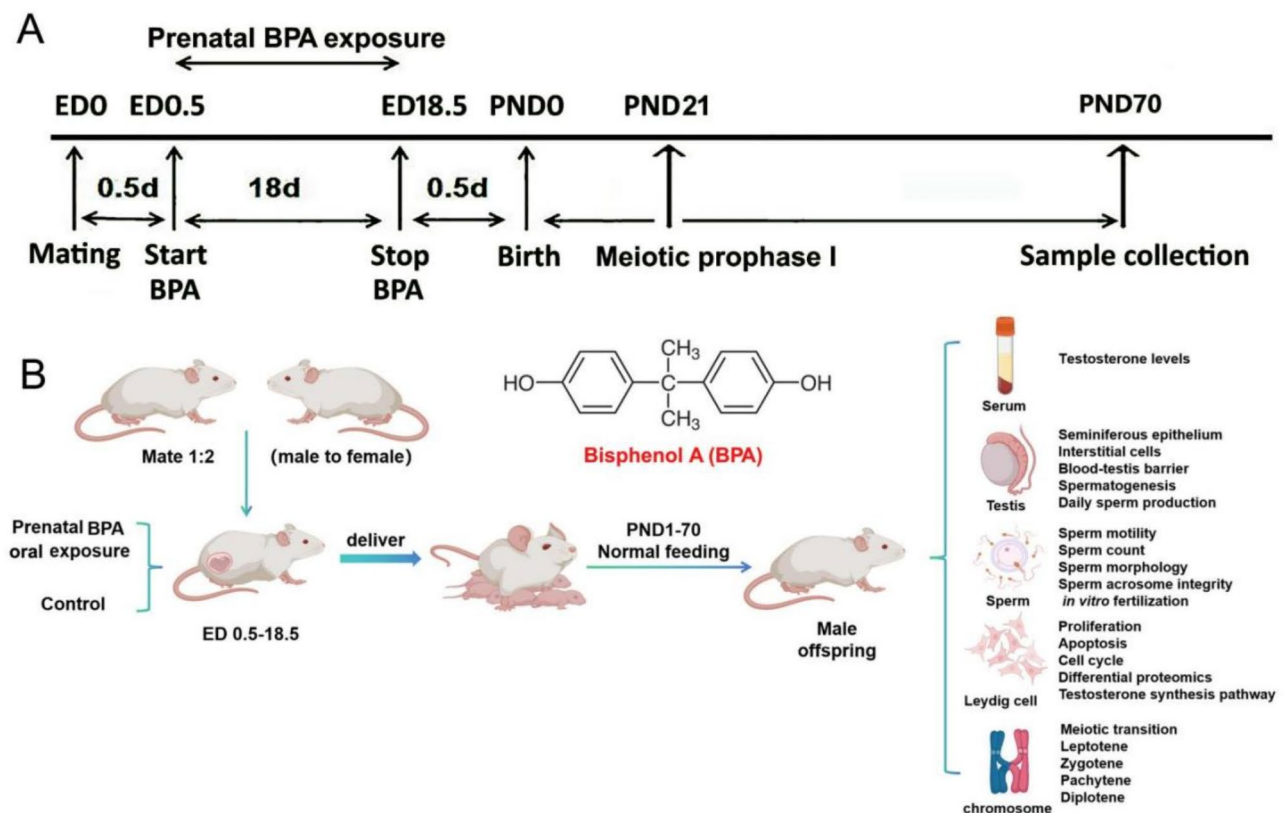


**Fig. 1.** Experimental design of prenatal exposure to BPA. **(A)** Diagram showing exposure timelines and procedures. **(B)** Adult male and female mice were allowed to mate at a 2:1 female to male ratio. Pregnant mice were exposed with BPA (50 mg/kg/day) via intragastric injection from embryonic day (ED) 0.5 to 18.5. The male offspring mice were anatomized at postnatal day (PND) 70. The diagrams show experimental workflow of this study. The figure was made by using Biorender system ([www.biorender.com](http://www.biorender.com)).

### Testicular histology and chromosome spread analyses

Testicular morphology was examined using hematoxylin and eosin (HE) staining, a widely accepted method for assessing tissue morphology under a light microscope (DM LB2, Leica, Nussloch, Germany). To determine the percentage of stage VII and stage VIII tubules, at least 30 circular tubules were counted in each section, and the percentage of stage VII and stage VIII were calculated separately<sup>21</sup>. For nuclear spread analysis, germ cells from PND 21 testes were collected using a previously described method<sup>22</sup>. The antibodies used for spread analysis were as follows: anti-Sycp3 (1:100; 23024-1-AP, Proteintech), and anti-H2ax (1:100; AG2114, Beyotime).

### Quantitative reverse transcription PCR (RT-qPCR)

Briefly, RNA extraction was performed using Trizol reagent (R701-01, Vazyme, Nanjing, China). After synthesizing cDNA from total RNA by using 5 × All-In-One RT MasterMix with AccuRT (G592, Abm, Jiangsu, China), RT-qPCR was conducted with BlasTaq 2 × qPCR MasterMix (G891, Abm, Jiangsu, China) on an ABI Prism 7500 (Thermo Fisher Scientific, Shanghai, China). Each sample was analyzed in triplicate. The relative mRNA expression levels were calculated using the  $2^{-\Delta\Delta Ct}$  method. The primer sequences are listed in Table 1.

### Immunohistochemical analysis

For immunohistochemical staining, the sections were blocked with 3% bovine serum albumin (BSA) and incubated with primary antibody (Cyp11a1, Pcn, Sycp3, Vimentin) at 4°C overnight, and with secondary antibody at RT for 1 h, staining with DAB Kit (ZLI-9018, Zhongshan Golden bridge, Beijing, China) and Harris hematoxylin solution (ZLI-9609, Zhong-Shan Golden bridge, Beijing, China). The stained sections were observed under a light microscope (DM LB2, Leica).

### TUNEL assay

A one-step TUNEL apoptosis assay kit (Beyotime Biotechnology, China) was used to detect apoptotic cells that underwent extensive DNA degradation. The results were observed by fluorescence microscopy (ZEISS, Axio Observer 7, Germany).

Gene symbol	Official full name	NCBI Gene ID	Primer sequence(5' to 3')
Actb	actin, beta	11,461	Forward: ACCTTCTACAATGAGCTGCG
			Reverse: CCTGGATAGCAACGTACATGG
Cyp11a1	cytochrome P450, family 11, subfamily a, polypeptide 1	13,070	Forward: TCAAAGCCAGCATCAAGGAG
			Reverse: CTAGCCACCTGTACCAAGTCT
Cyp17a1	Cyp17a1 cytochrome P450, family 17, subfamily a, polypeptide 1	13,074	Forward: AGAGTTTGCCATCCCGAAG
			Reverse: AACTGGGTGTGGGTGTAATG
Hsd3b1	hydroxy-delta-5-steroid dehydrogenase, 3 beta- and steroid delta-isomerase 1	15,492	Forward: ATTCCGACCAGAAACCAAGG
			Reverse: AGAATGTCTCTTCCAACACTG
Star	steroidogenic acute regulatory protein	20,845	Forward: GAAGCTCCTATAGACATATGCGG
			Reverse: GAAGTTGACCCATCCACCC
Hsd17b3	hydroxysteroid (17-beta) dehydrogenase 3	15,487	Forward: CTTCGTCCTGGCCTCTTTA
			Reverse: TTCAGCTCCGATCGTGACAT

**Table 1.** Primers used for quantitative real-time PCR.

**Western blotting**

Testicular proteins were extracted using a Radio Immunoprecipitation Assay (RIPA) buffer (P0013, Beyotime, Shanghai, China). Protein concentrations were measured using a BCA protein assay kit (P0012, Beyotime, Shanghai, China). Each sample was loaded onto 12% SDS-PAGE gels, transferred onto a nitrocellulose membrane. The membranes were incubated with primary antibodies (BAX, ab32503; BCL2, ab182858, abcam). The resultant membranes was incubated with appropriate HRP-conjugated secondary antibody (ZB2305, Zhong-Shan Golden bridge, Beijing, China) and detected by an ECL kit (KF8001, Affinity Biosciences, Jiangsu, China) using ChemiScope 6200 Touch (CLINX Science Instruments Co., Ltd. China). The protein bands were quantified with ImageJ software using ACTB as the loading control.

**Cell counting Kit-8 (CCK8) assay**

Cell counting Kit-8 (CCK8) assay Leydig cells were plated in 96-well plates at 10000 cells/well. Cell were treated with various concentrations(0, 50, 100, 200, 400, 600, 800, 1000, and 1200  $\mu$ M in 0.1% DMSO) of BPA, for 24–48 h in DMEM-F12 medium. Each sample was measured using a CCK8 kit (Dojindo, CK04, Japan) according to the manufacturer’s protocol. The data were analyzed by a online IC50 Calculator (<https://www.aatbio.com/tools/ic50-calculator>).

**Flow cytometry and cell cycle analyses**

Leydig cells planting in 6-well plates at 150 $\mu$ M BPA in 0.1% DMSO for 48 h were used for treating cells in DMEM-F12 medium. FITC Annexin V Apoptosis Detection Kit I (BD Biosciences, San Jose, CA, USA) was used for flow cytometry analysis of apoptosis according to the manufacturer’s protocol. Flow cytometry analysis of the cell cycle and apoptosis on control and BPA treated Leydig cells was performed on a Moflo XDP flow cytometer (Beckman Coulter, Brea, CA, USA)<sup>23</sup>.

**Quantitative proteome analysis of BPA-exposed mice Leydig cell**

Leydig cells were cultured in 6-well plates with 150 $\mu$ M BPA in 0.1% DMSO for 48 h and subsequently subjected to proteome analysis using a hybrid data-independent acquisition (DIA) strategy. Briefly, proteins were digested into peptides, which were then separated by a nanoflow reversed-phase high-performance liquid chromatography (Easy nLC1200, Thermo Fisher) coupled to an Orbitrap Q-Exactive HF mass spectrometer (Thermo Fisher Scientific, Waltham, MA) operating in HCD fragmentation mode. Bioinformatics analysis was performed on the identified differentially expressed proteins. The Gene Ontology (GO) analysis was conducted using online bioinformatics tools from the Database for Annotation, Visualization and Integrated Discovery (DAVID) tools (<https://david.ncifcrf.gov>), and protein-protein association networks were generated using the STRING database (<https://string-db.org>). The figures were created using Biorender system ([www.biorender.com](http://www.biorender.com)).

**Statistical analysis**

All data are presented as the mean  $\pm$  standard deviation (SD) from three independent experiments. Statistical analyses were performed using student’s t-test. All analyses were conducted using GraphPad Prism 8 (GraphPad Prism, La Jolla, CA). a p-value less than 0.05 was considered statistically significant.

**Results**

**SubsectionPrenatal BPA exposure altered genital tract morphology, testis histology and serum testosterone concentration in offspring male mice**

We constructed a prenatal BPA-exposed mouse model and analyzed the male genital tracts of the male offspring (Fig. 1) Morphological analysis revealed significant alterations in the male genital tracts of offspring mice exposed maternally to BPA during pregnancy. The seminal vesicles (SV), vas deferens (VD), and epididymises (EP) of BPA-exposure offspring mice were significantly atrophied. The testes (T) were also reduced in size. PA exposure had no effect on the number of offspring but significantly decreased their body weight, testicular weight, sperm

count, and daily sperm production (Fig. 2A). The seminiferous tubules in control mice were uniformly in shape and closely arranged. Leydig cells (Lc) in the interstitial space of the seminal tubules, spermatogonias (Sp), spermatocytes (Ps), round spermatids (Rs), and elongated spermatids (Es) were observed in the tubules, in contrast, in prenatal BPA-exposed offspring, germ cells in spermatogenic tubules of all stages were decreased and arranged loosely. In prenatal BPA-exposed offspring, the proportions of stage VIII tubules in the prenatal BPA-exposed mice were significantly reduced. The intercellular space were increased, and the number of Leydig cells was significantly decreased from 19.11 to 10.04%. Moreover, the serum testosterone level also decreased significantly from 9.993(ng/ml) to 7.29(ng/ml) (Fig. 2B).

### **Prenatal BPA exposure Lowered offspring sperm motility, morphology, acrosome integrity and fertility in male mice**

Morphological analysis of sperm revealed that prenatal BPA exposure dramatically increased the proportion of headless sperm from 10.96 to 14.79% in male offspring mice (Fig. 3A). Prenatal exposure to BPA also significantly reduced the proportion of sperm with intact acrosomes from 85.93–77.98% (Fig. 3B). These findings aligns with findings from studies indicating that BPA exposure during the lactation period can lead to decreased sperm motility and increased abnormal sperm morphology in adult male mice. Cauda epididymal sperm from prenatal BPA-exposed offspring mice were collected to examine their effect on sperm quality. The sperm motility and velocity parameters, as assessed by the CASA system revealed that total and progressive motilities, curvilinear velocity (VCL), straight velocity (VSL), velocity average path (VAP), and lateral head displacement (ALH) were significantly decreased in prenatal BPA-exposed offspring mice. In contrast, linearity (LIN) and straightness (SRT) were higher in BPA exposed mice, while beat cross frequency (BCF) was not affected by prenatal BPA exposure (Fig. 3C).

Exposure to Bisphenol A (BPA) can adversely affect male fertility, as evidenced by studies showing decreased sperm count and increased sperm abnormalities in male mice exposed to BPA during adolescence. Fertility of prenatal BPA-exposed offspring was further evaluated *in vitro*. The outcome of the *in vitro* fertilization (IVF) experiment showed prenatal BPA exposure decreased the fertilization rate of male offspring. Compared to the control group, prenatal exposure to BPA significantly decreased the percentage of sperm binding per oocyte from 17.83 to 12.53%, the percentage of two-cell stage embryos from 84.77 to 57.77%, and the percentage of eight-cell stage embryos from 59.53 to 34.20% during early embryo development (Fig. 4). These results are consistent with findings from studies that have shown BPA exposure can lead to reproductive health issues and negatively impact embryo development.

### **Prenatal BPA exposure arrested meiotic transition from Zygotene to pachytene spermatocytes in offspring male mice**

To further analyze the effects of prenatal BPA exposure on male mice offspring, the processes of chromosomal synapsis and meiotic recombination were examined by immunostaining axial element protein (Sycp3) and  $\gamma$ H2AX in spread nuclei. During the leptotene and zygotene stages, SYCP3 assembled normally into the lateral elements of synaptonemal complexes in spermatocytes of offspring exposed to prenatal BPA, similar to the control group. The periodic change in the phosphorylation distribution of H2AX during meiotic prophase I is one of the hallmark events of meiosis. In male mice, there are three waves of H2AX phosphorylation signal amplification during meiotic prophase I. Leptotene stage: the first wave of H2AX phosphorylation occurs at this stage, mediated by ATM and independent of programmed DNA double-strand break (DSB). The  $\gamma$ H2AX signal is primarily distributed along the chromosome axis. Zygotene phase: The second wave of H2AX phosphorylation occurs, mediated by ATR and dependent on programmed DSB. At this stage, the  $\gamma$ H2AX signal spreads from the chromosome axis to the entire nucleus region. Pachytene and Diplotene stages: The third wave of H2AX phosphorylation occurs, also mediated by ATR but not dependent on DSB. The  $\gamma$ H2AX signal is mainly distributed in the non-synapsed chromosomal regions, particularly in the sex vesicle regions of the sex chromosomes. We observed no difference in these three waves between the control and prenatal BPA-exposed offspring (Fig. 5A). Prenatal exposure to BPA resulted in a notable increase in the percentage of zygotene spermatocytes to 26.50% in the offspring, compared to 12.44% in the control group (Fig. 5B). This finding aligns with studies showing that BPA can influence male reproductive cell development and function.

### **Detection of male germ cell specific proteins in prenatal BPA- exposed offspring male mice**

We further analyzed whether prenatal BPA exposure altered the expression of key marker proteins associated with spermatogenesis in male offspring. In the testes, the level of protein Pcn1 is related to the proliferation of germ cells, the level of protein Sycp3 reflects the process of meiosis, the level of protein Vimentin reflects the development of blood-testis barrier (BTB), and protein Cyp11a1 level is associated with androgen synthesis.

Prenatal BPA exposure led to decreased expressions of Pcn1, Sycp3, and Vimentin in testicular seminiferous epithelium, and significantly decreased expressions of Cyp11a1 in testicular Leydig cells, indicating impaired development and secretory function (Fig. 6). The TUNEL assay was used to evaluate apoptotic germ cells in male offspring mice maternally exposed to BPA during pregnancy. Compared with the control group, the number of TUNEL-positive cells significantly increased in the testes of BPA-exposed offspring, and the positive cells primarily located in Leydig cells (Fig. 7A). The western blot showed that the expression of anti-apoptotic protein BCL2 was downregulated, and the pro-apoptotic protein BAX was upregulated. Prenatal BPA exposure significantly increased the BAX/BCL2 ratio in the offspring testes, consistent with the TUNEL assay results (Fig. 7B).



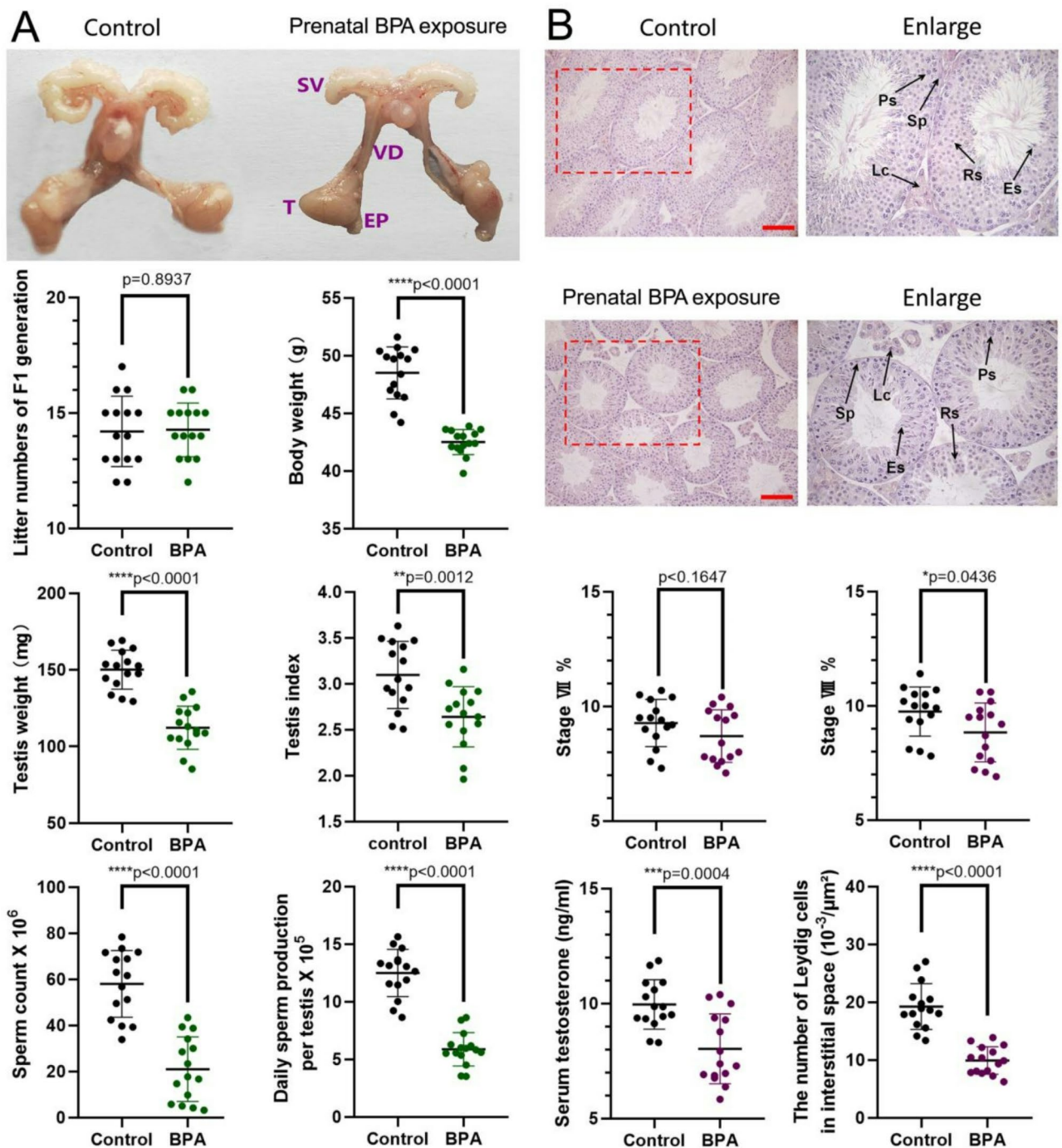


**Fig. 2.** Morphology and histology of the male genital tracts of prenatal BPA-exposed mice offspring. Morphology of the male genital tracts of control and prenatal BPA-exposed mice offspring (A). T (testis), SV (seminal vesicle), VD (vas deferens), EP (epididymis). Litter numbers of F1 generation in control and BPA-exposed pregnant mice. Characteristics of body weight, testis weight, testicular index, sperm count and daily sperm production in control and prenatal BPA-exposed offspring. (B) Histopathology of testes of control and prenatal BPA-exposed offspring. The sections were demonstrated by HE staining. Sp (spermatogonia), Ps (spermatocyte), Rs (round spermatid), Es (elongated spermatids), Lc (leydig cells). Percentages of testicular stage VII and VIII tubules. The number of Leydig cells in interstitial space in control and prenatal BPA-exposed offspring. Testosterone concentration in control and prenatal BPA-exposed offspring. Each bar represented 100  $\mu m$ . The data were analyzed by t-test,  $p < 0.05$  was considered significance. Each bar represented 100  $\mu m$ .

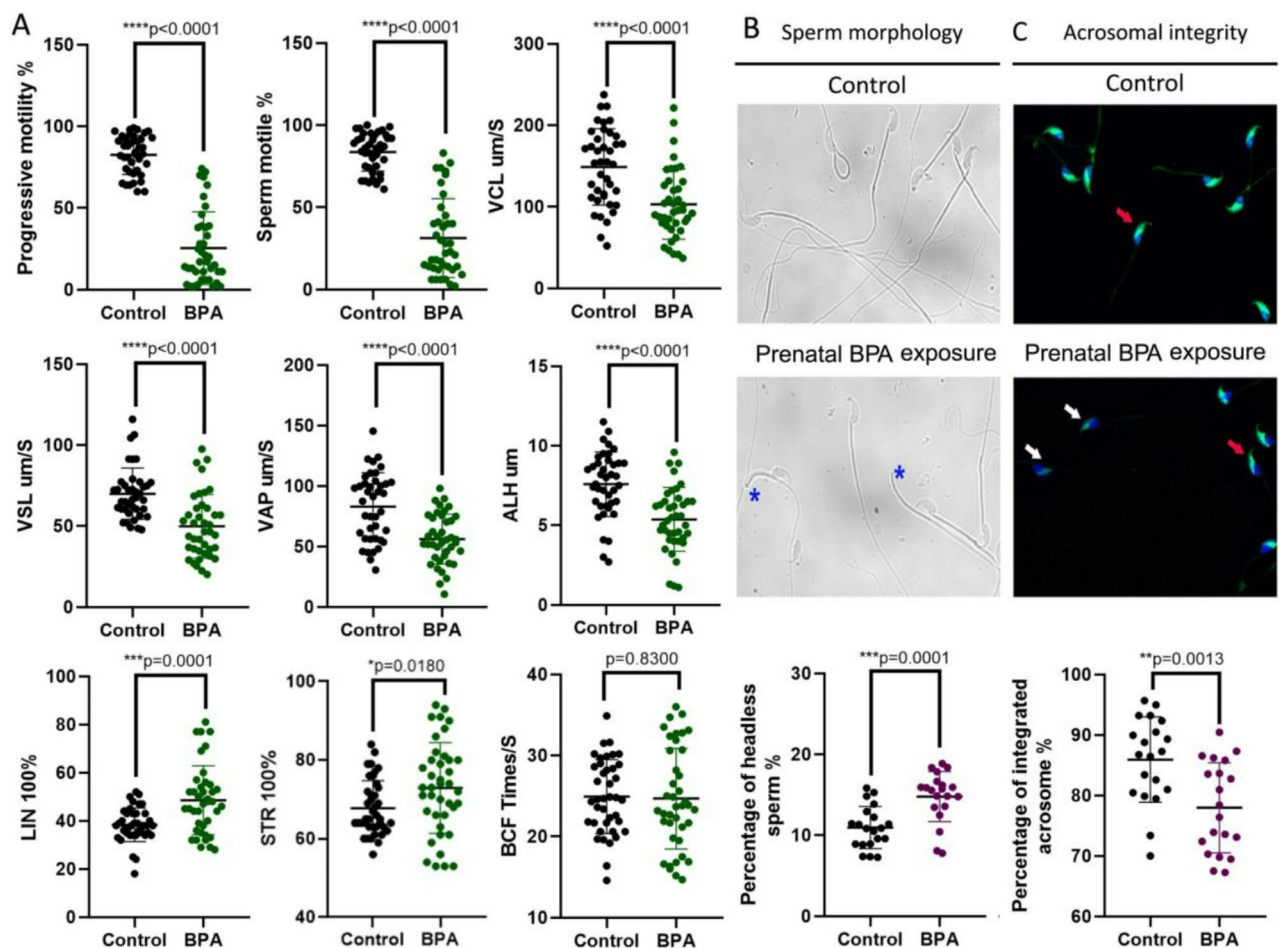


**Fig. 3.** Analysis of sperm motility, sperm morphology and acrosome integrity in control and prenatal BPA-exposed offspring. **(A)** Sperm motility of control and prenatal BPA-exposed offspring. VCL (curvilinear velocity), VSL (linear velocity), VAP (velocity average path), ALH (lateral head displacement), LIN (linearity), STR (straightness), BCF (beat-cross frequency). **(B)** Sperm morphology of control and prenatal BPA-exposed offspring. Blue asterisk showed headless sperm. **(C)** Sperm acrosome integrity of control and prenatal BPA-exposed offspring. Red arrow indicated integrated acrosome, and white arrow showed non-integrated acrosome. The blue staining was the nucleus stained by DAPI, and the green signals showed acrosome. Each bar represented 50  $\mu\text{m}$ . The data were analyzed by t-test,  $p < 0.05$  was considered significance.

### BPA inhibited the proliferation of Leydig cell in vitro

Because prenatal BPA exposure caused the most severe damage to Leydig cells and most significantly reduced the expression of the protein Cyp11a1 in male mice offspring, we further examined the effect of BPA on the proliferation. Leydig cells were treated with various concentrations of BPA (0, 50, 100, 200, 400, 600, 800, 1000, and 1200  $\mu\text{M}$  in 0.1% DMSO) for 24–48 h. As shown in Fig. 8, the proliferative ability of Leydig cells decreased in a dose-dependent manner. The IC<sub>50</sub> values of BPA exposure in Leydig cells were 223.15  $\mu\text{M}$  for 24 h and 177.61  $\mu\text{M}$  for 48 h. The results demonstrated that the survival rate of Leydig cells decreased with increasing BPA concentration, verifying a concentration-dependent inhibitory effect on Leydig cells proliferation (Fig. 8A). Furthermore, we determined whether BPA could induce cell cycle arrest in Leydig cells in vitro. Cells were exposed to various concentrations of BPA (0, 50, 100, 150, and 200  $\mu\text{M}$ ) for 48 h, and DNA content was analyzed by flow cytometry. BPA treatment increased the proportion of cells in the G<sub>0</sub>/G<sub>1</sub> phase from 64.01 to 84.64%, while reducing the number of cells in the G<sub>2</sub>/M-phase from 25.21 to 8.00%. BPA also decreased the proportion of S-phase cells from 10.78 to 7.36%. The inhibitory effect of BPA on Leydig cell proliferation appears to be primarily associated with G<sub>0</sub>/G<sub>1</sub> cell cycle arrest, as indicated by observed changes in the expression of proteins GR, 11 $\beta$ -HSD, and StAR in rats (Fig. 8B).

To ascertain the involvement of the apoptotic pathway in BPA-induced cytotoxicity in Leydig cells, an Annexin V/PI double staining assay was conducted, and the results were analyzed using flow cytometry. The flow cytometry data were represented in a quadrant diagram, with Q1 indicating necrotic cells, Q2 representing late apoptotic and dead cells, Q3 depicting early apoptotic cells, and Q4 indicating normal cells. Leydig cells were exposed to various concentrations of BPA (0, 50, 100, 150, and 200  $\mu\text{M}$ ) for 48 h, and the apoptosis effects were analyzed. The results showed that BPA significantly promoted apoptosis in Leydig cells in a dose-dependent

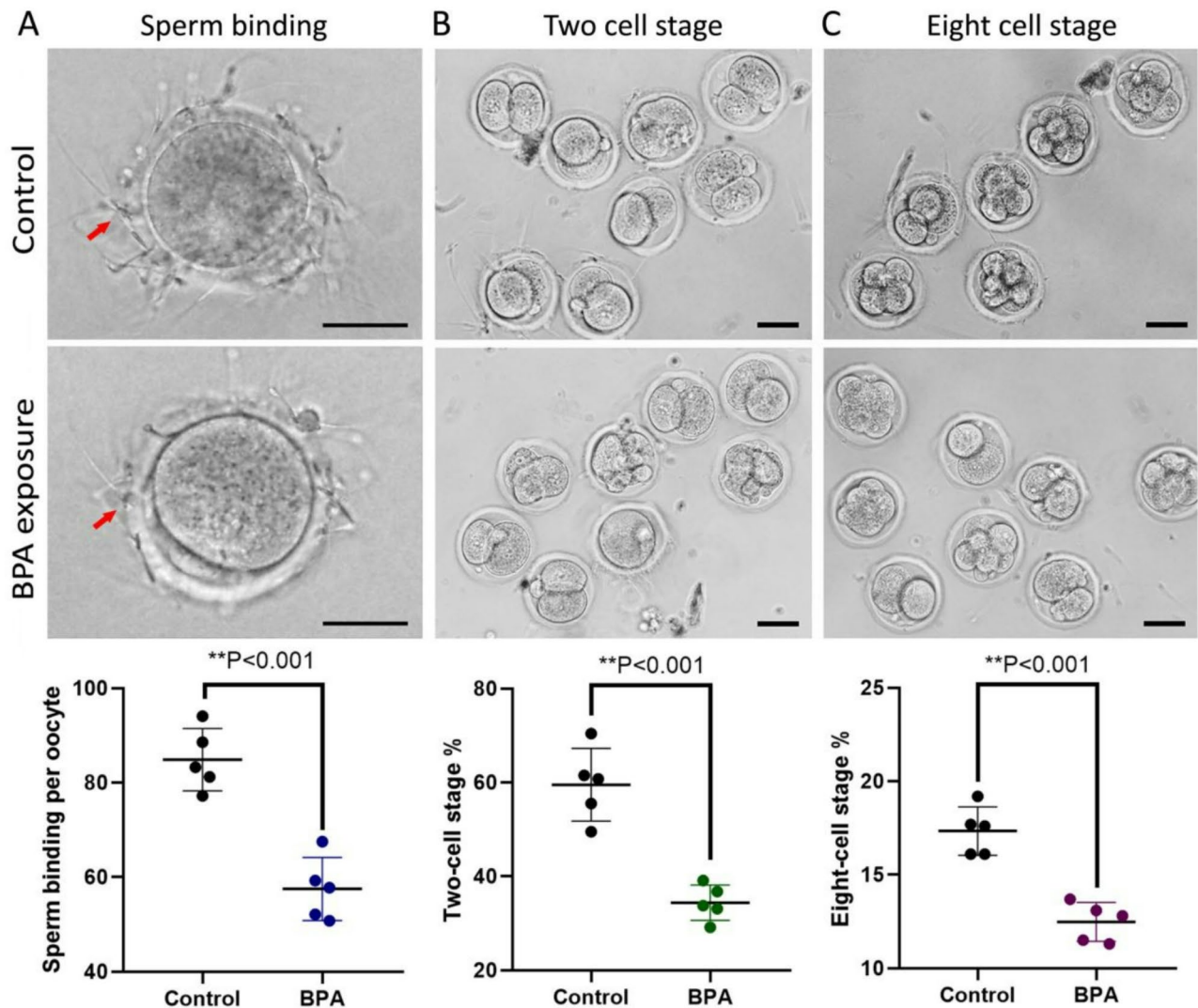


**Fig. 4.** The male fertility of prenatal BPA-exposed offspring by IVF analysis. Sperm binding ability was displayed as the average number of sperm binding with one oocyte, and the arrow indicated the binding sperm. The two-cell stage rate was displayed as the number of two-cell embryos / the number of pronucleus formation oocyte. Eight-cell stage rate was displayed as the eight-cell embryos / the number of the two cell embryos. Each bar represented 100  $\mu$ m. The data were analyzed by t-test,  $p < 0.05$  was considered significance.

manner, characterized by a significant increase in apoptosis (Q2 plus Q3: early plus late apoptosis) compared to the control group (Fig. 8C).

#### Differentially expressed Leydig cells proteins induced by BPA exposure in vitro

Quantitative proteomics was performed using label-free methods on Leydig cells exposed to 150  $\mu$ M BPA for 48 h. Proteins were extracted from the cells, digested by trypsin, and further identified. A total of 234 differentially expressed proteins (DEPs) were identified, including 97 proteins that were downregulated and 137 proteins that were upregulated in the BPA-exposed group (Supplemental Table 1). Bioinformatics enrichment analysis of molecular functions based on Gene Ontology (GO) annotation showed that estrogen response element binding was prominently present in the proteins downregulated following BPA exposure. Key biological processes affected by BPA treatment included centrosome duplication and apoptotic regulation, which showed marked alterations in their associated protein expression profiles. These downregulated proteins were primarily localized to transcriptional regulatory complexes, particularly within transcription factor complexes and Cajal bodies. Conversely, upregulated proteins in BPA-exposed Leydig cells demonstrated enrichment in metabolic pathways including lipid metabolism, oxidative detoxification, and reactive oxygen species (ROS) metabolism (Fig. 9). Critical validation of testosterone biosynthesis pathway components demonstrated significant BPA-induced down-regulation at molecular level. Key steroidogenic enzymes including cytochrome P450 family members (Cyp11a1 and Cyp17a1), hydroxysteroid dehydrogenases (Hsd3b1 and Hsd17b3), and the steroidogenic acute regulatory protein (StAR) showed substantial decreases in expression (Fig. 10).



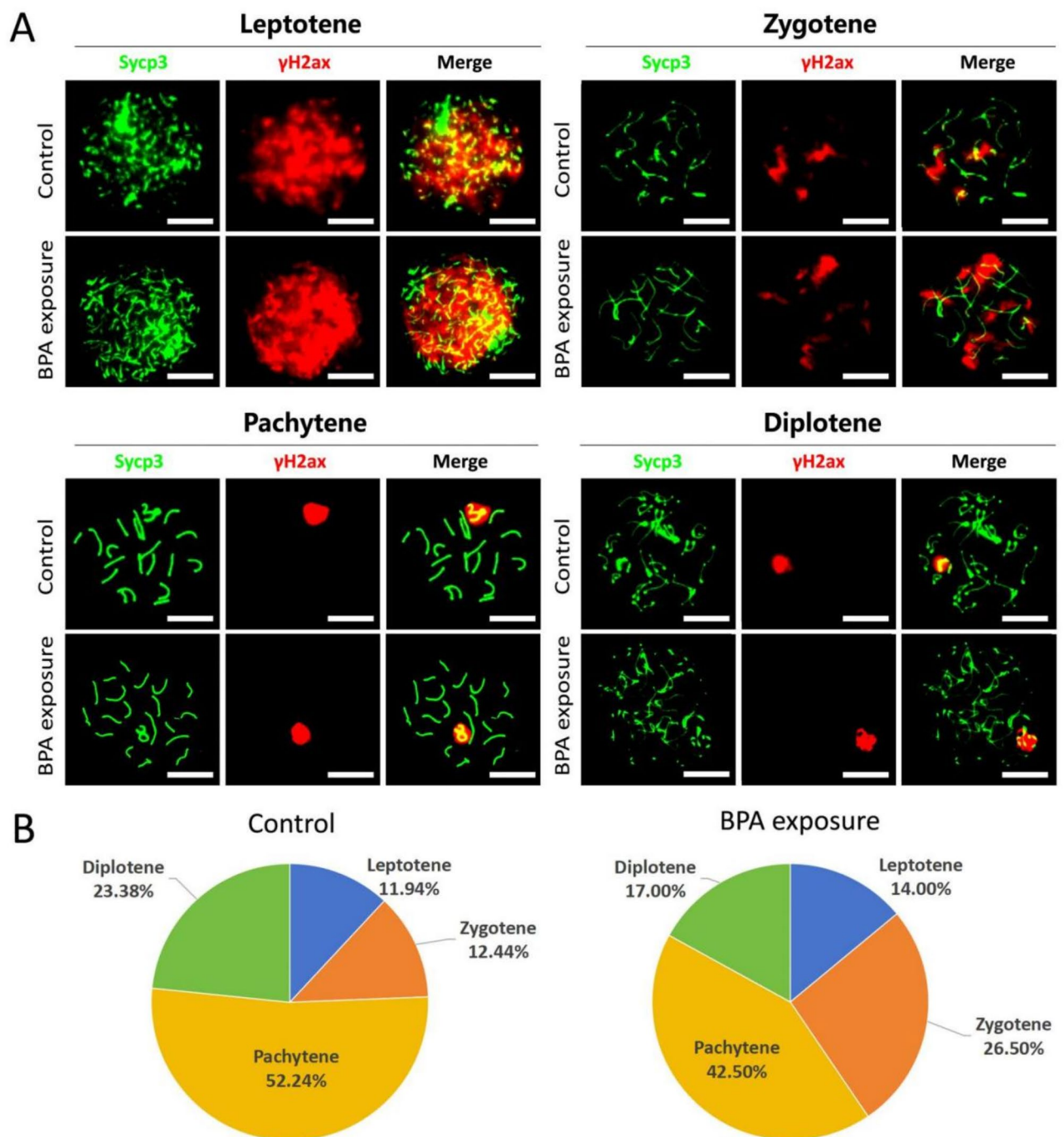


**Fig. 5.** Prenatal BPA-exposed offspring mice disturb meiotic transition from zygotene to pachytene spermatocytes. **(A)** Immunofluorescence staining for Sycp3 (green) and  $\gamma$ H2ax (red) in control and prenatal BPA-exposed offspring spermatocytes. **(B)** The ratio of meiotic spermatocytes at the indicated stages in control and prenatal BPA-exposed offspring. Ten fields of view were randomly selected from each testes for counting. Each bar represented 20  $\mu$ m.

## Discussion

Bisphenol A (BPA), a well known endocrine disruptor, adversely affects male reproductive function. Numerous toxicological and epidemiological studies have reported inconsistent results, likely due to variations in experimental conditions such as animal age, exposure dosage, route of administration, and duration of exposure. For instance, fetal or perinatal exposure to BPA has been linked to abnormal offspring development, including potential issues with brain development and behavior<sup>24</sup>. Exposure to BPA in utero adversely affects fetal male reproductive development and cord blood estradiol levels, increasing the risk of urogenital developmental abnormalities (e.g., hypospadias, cryptorchidism, histological alterations of the fetal testes)<sup>25</sup>. It also significantly

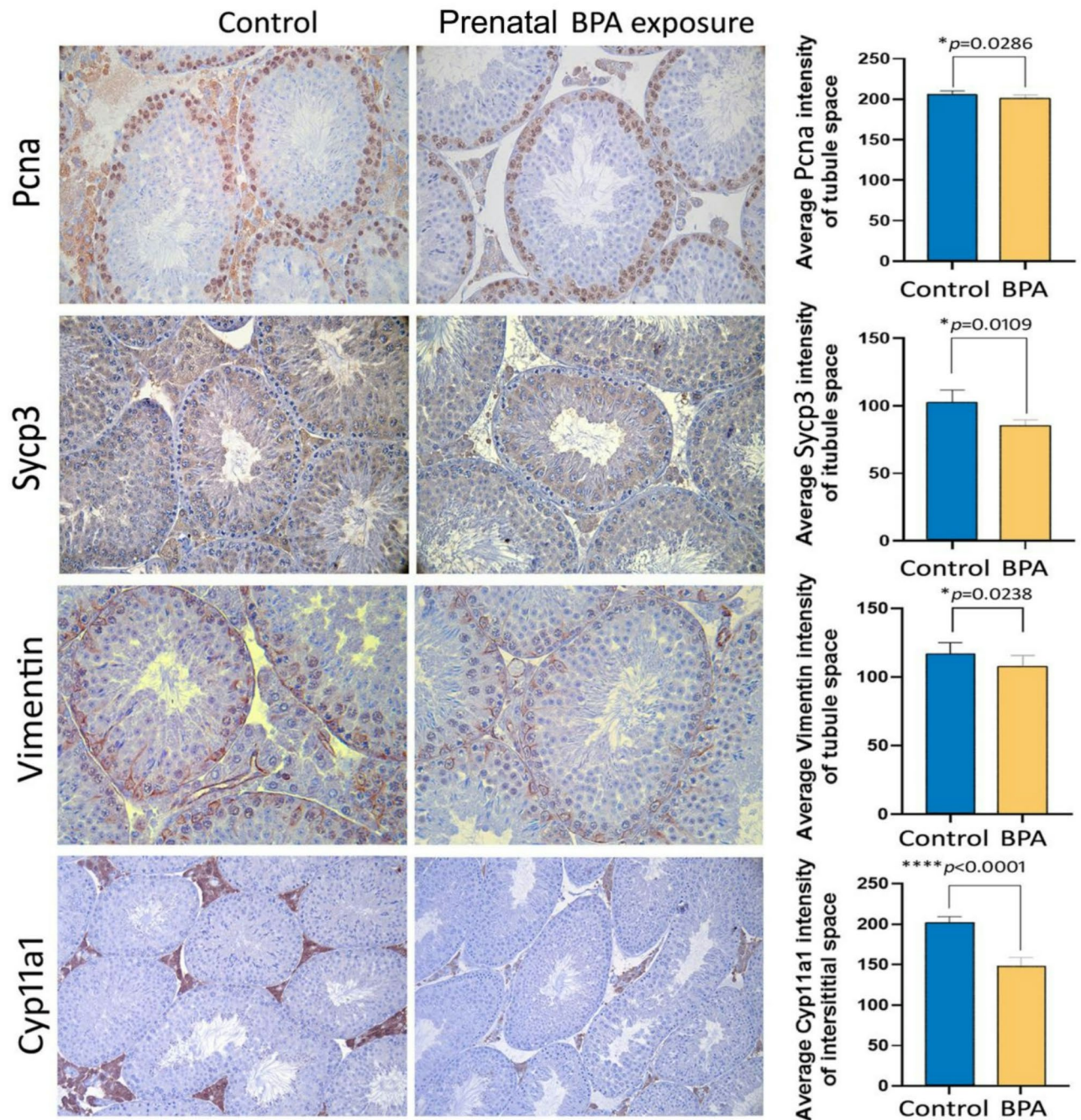


**Fig. 6.** Impact of prenatal BPA exposure on the expression of proteins related to spermatogenesis in the testes of male offspring mice. Protein expression of PCNA, SYCP3, Vimentin and Cyp11a1 in mice testis from control and prenatal BPA-exposed offspring by IHC analysis. Ten fields of view were randomly selected from testes of each experimental group for counting, each bar represented 50  $\mu$ m. The data were analyzed by t-test,  $p < 0.05$  was considered significance.

alters birth weight and urethra sinus (UGS) morphology, including an increased size of the colliculus and a decreased size of the urethra<sup>26</sup>. In this study, we constructed a prenatal BPA-exposed offspring mice model. Pregnant mice were administered BPA (50 mg/kg/day) via intragastric injection from embryonic day (ED) 0.5–18.5. Our aim was to determine the harmful effects of BPA on key biological processes of spermatogenesis in the intergenerational transmission.

Prenatal BPA exposure significantly reduced birth weight in offspring, indicating impaired fetal growth and morphological development<sup>26</sup>. The testicular coefficient, a measure of testicular weight relative to body weight, serves as an indicator of testicular health and BPA-induced toxicity. In our previous study, we found no significant difference in testicular quality after exposure to BPA in adult mice<sup>19</sup>. However, other studies



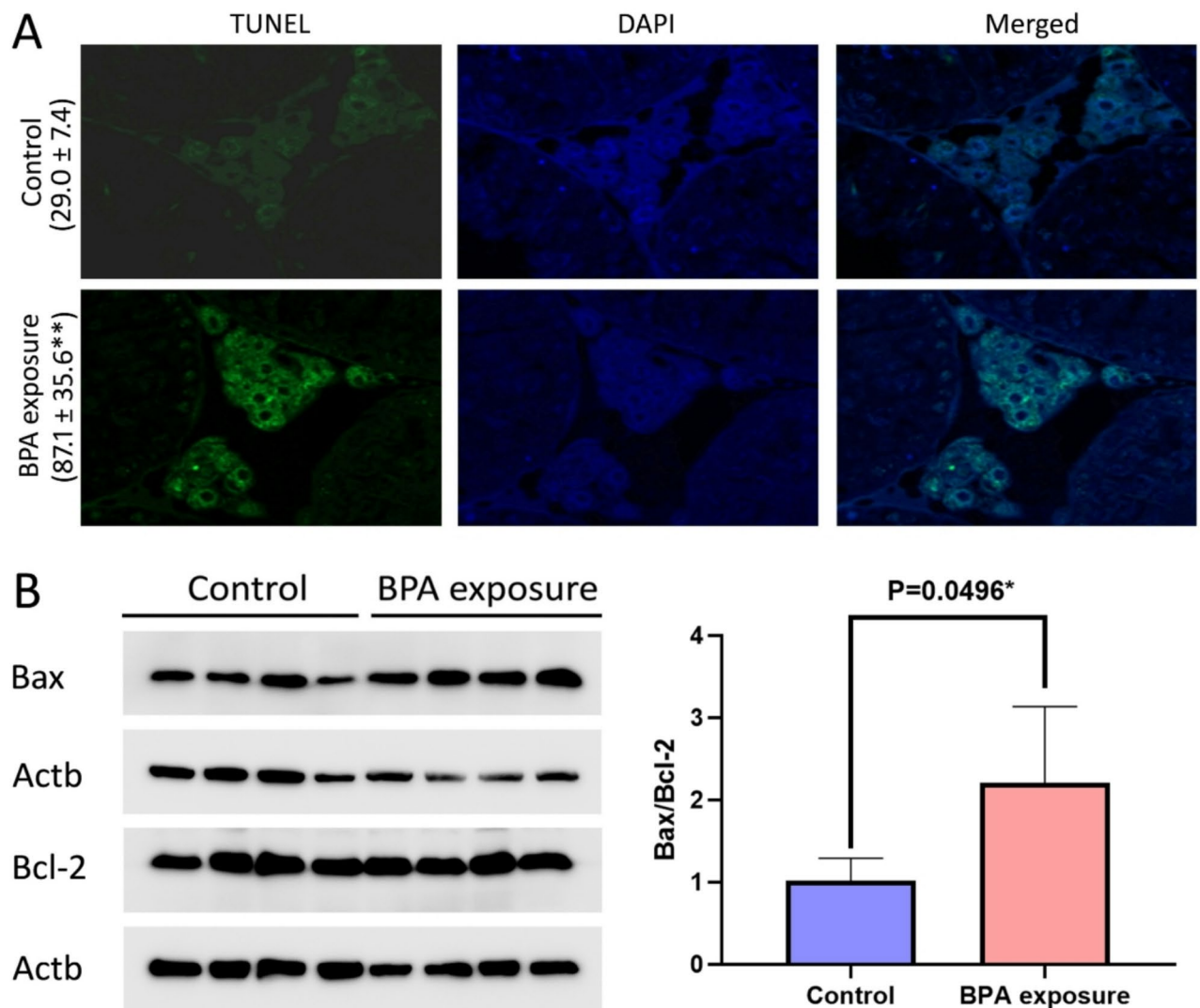


**Fig. 7.** Apoptosis detection by TUNEL assay and expression of BAX/BCL-2 of control and prenatal BPA-exposed offspring testes. **(A)** TUNEL assay in control and prenatal BPA-exposed offspring testes. The blue staining was the nucleus stained by DAPI, and the green signals were the apoptotic cells. **(B)** Western blot analysis of BAX/BCL-2 in control and prenatal BPA-exposed offspring testes with triple replications. Each bar represented 50  $\mu$ m. The data were analyzed by t-test.  $p < 0.05$  was considered significance (Supplemental Fig. 1).

have shown that BPA exposure can lead to significant changes in the reproductive system of mice, including decreased sperm quality and increased DNA damage in testicular cells. This research found that exposure to BPA during pregnancy did not result in a reduction in litter size, but there was a trend toward decrease in body weight, testicular wet weight, and testicular index in male offspring mice maternally exposed to BPA during pregnancy. We inferred that maternal exposure to BPA during pregnancy does not result in embryonic death but affects reproductive development<sup>27</sup>. However, prenatal BPA exposure did not significantly alter seminiferous tubule morphology, except for a marked reduction in stage VIII tubules—a finding consistent with our previous observations in adult mice chronically exposed to BPA<sup>19</sup>.

Prenatal BPA exposure altered key spermatogenesis-related molecules associated with germ cell proliferation (Pcna), meiosis (Sycp3), blood-testis barrier (Vimentin), and testosterone production (Cyp11a1) in the testes of male offspring. The results indicated that prenatal BPA exposure reduced the expression of Pcna, Sycp3, and Vimentin, and markedly decreased the expression of Cyp11a1 in testicular Leydig cells, suggesting potential impairment in developmental processes and testosterone secretion in prenatal BPA exposed offspring. Sperm motility is critical for male fertility<sup>28</sup>. Prenatal BPA exposure significantly reduced epididymal sperm motility parameters in offspring mice, including VCL (curvilinear velocity), VSL (linear velocity), VAP (velocity average path), and ALH (lateral head displacement). We evaluated the effects of prenatal BPA exposure on sperm fertility through in vitro experiments. Prenatal BPA-exposed offspring male mice exhibited reduced sperm-egg binding

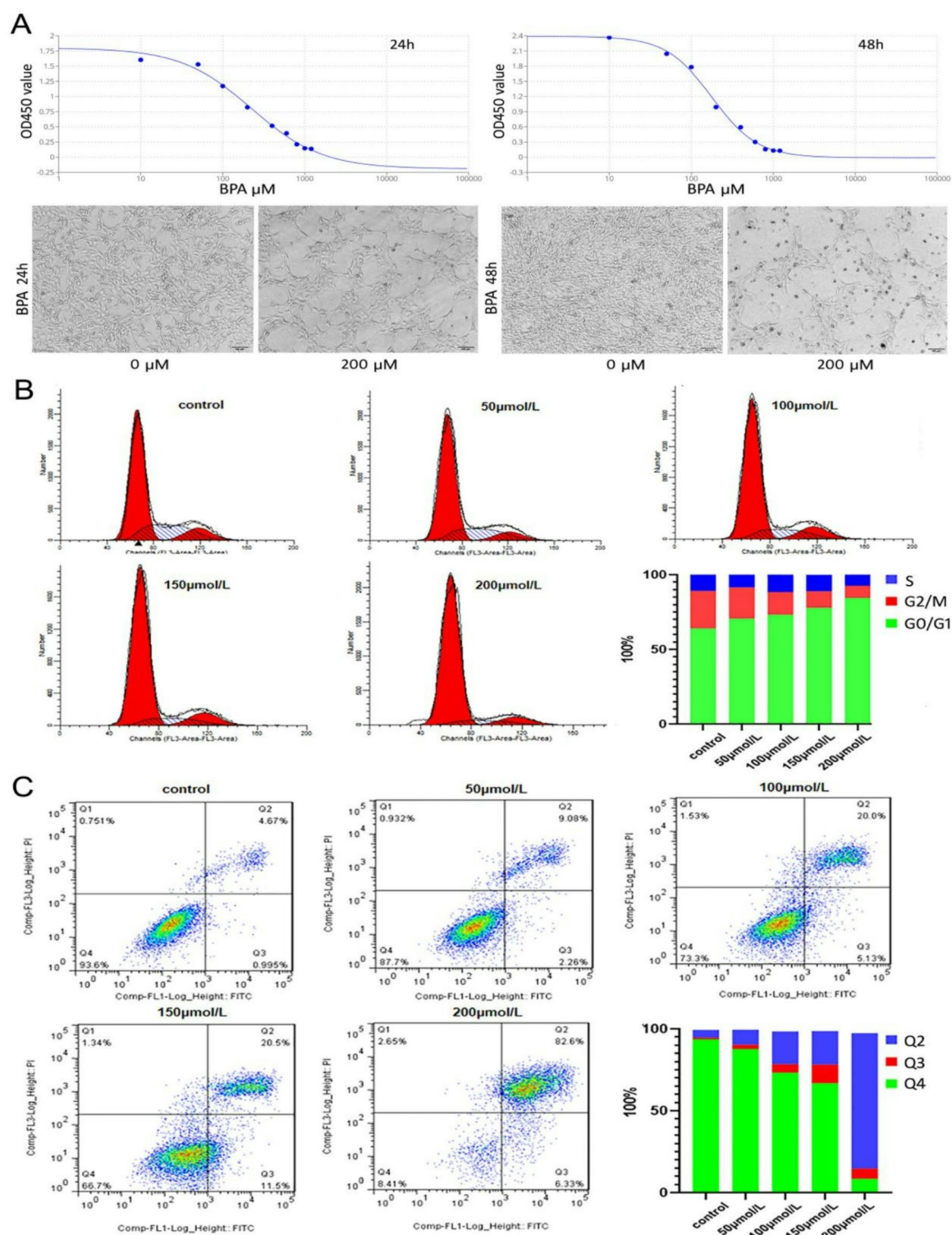


**Fig. 8.** The impact of various concentrations of bisphenol A (BPA) on the proliferation, apoptosis, and cell cycle progression in mouse Leydig cells. **(A)** Leydig cells were seeded in 96-wells plate with 10,000 cells/well, and were treated with various concentrations (0–1200  $\mu$ M) of BPA for 24 h and 48 h. Diluted DMSO was used as control. The CCK8 reagent was added, and the absorbance was measured at 450 nm wavelength with a microplate reader. **(B)** Leydig cells were exposed to varying concentrations of BPA (0, 50, 100, 150, and 200  $\mu$ M) for 48 h to assess the impact on their cell cycle progression. Following treatment, the cells were fixed and stained with propidium iodide (PI) for analysis using flow cytometry. The distribution and percentage of cells in G0/G1, G2/M, and S phase of the cell cycle were illustrated. **(C)** The cells were stained with FITC-annexin V and propidium iodide (PI). The original density plots of Flow Cytometry analysis were showed. The distribution and percentage of cells in sub Q1, Q2, Q3 and Q4 of the cell cycle are illustrated. Q1 (necrotic), Q2 (late apoptotic cells and dead cells), Q3 (early apoptotic cells), Q4 (Normal cells).



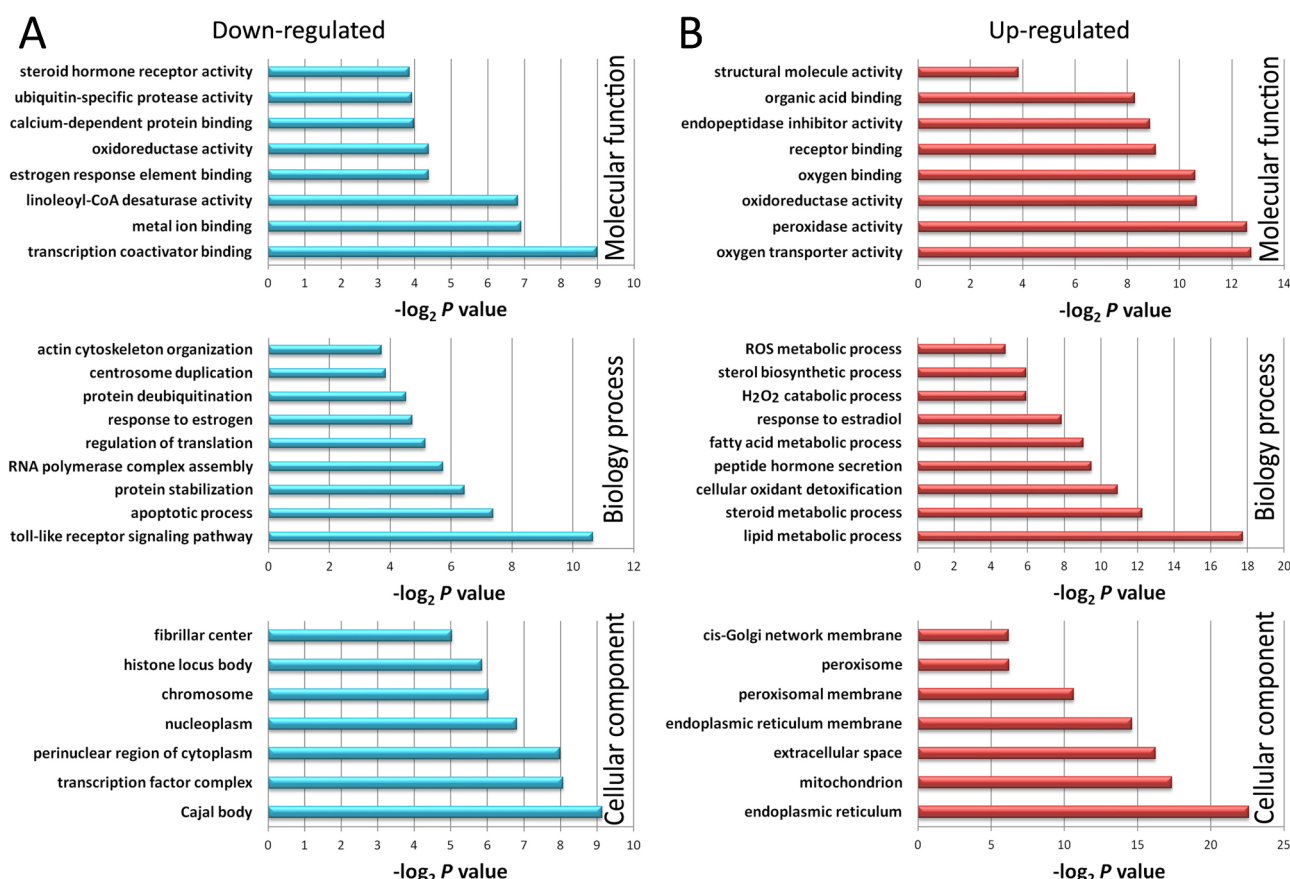


**Fig. 9.** Bioinformatic analysis of differential proteins induced by BPA exposure in Leydig cells. Over-representative analysis of molecular functions, biology processes, and cellular components of down-regulated (A) and up-regulated (B) proteins in BPA-exposed Leydig cell.

ability, and the formation rates of two-cells/eight-cells stages, suggesting that prenatal BPA exposure adversely affected offspring sperm quality and function.

To determine whether prenatal BPA exposure affects normal meiotic progression, we analyzed chromosome dynamics during meiotic prophase I. Specifically, we examined the process of chromosomal synapsis using immunostaining for axial element protein (SYCP3) and assessed the process of chromosomal recombination by immunostaining spread nuclei with  $\gamma$ H2AX. During the meiotic leptotene and zygotene stages, meiotic DNA double-strand breaks (DSBs) initiate homologous chromosomal synapsis, and SYCP3 was assembled on the synaptonemal complexes. The dynamics of  $\gamma$ H2AX distribution, which is typically considered a marker for meiotic progression<sup>29,30</sup>, were also examined. Our results showed that in both control group and prenatal BPA-exposed offspring, the initial two waves of  $\gamma$ H2AX staining expanded across the entire chromosomes during the leptotene and zygotene stages, while the third wave was restricted to the unsynapsed X and Y chromosome region (sex body) at the pachytene stage of meiosis. However, the percentage of zygotene spermatocytes was significantly higher in prenatal BPA-exposed offspring (26.50%) compared to controls (12.44%). This excessive accumulation of zygotene spermatocytes in prenatal BPA-exposed offspring is speculated to disrupt the normal progression of meiosis, specifically the transition from zygotene to pachytene spermatocytes. Consequently, these changes led to a reduction in the number of stage VIII seminiferous tubules in prenatal BPA-exposed mice.

Leydig cells play a crucial role in synthesizing androgens, primarily testosterone, from cholesterol. Testosterone directly participates in the regulation of spermatogenesis processes<sup>31,32</sup>. Prenatal exposure to BPA increases apoptosis in Leydig cells of the testes in male offspring mice, up-regulated pro-apoptotic protein BAX, and down-regulated the anti-apoptotic protein BCL-2. We also found a decrease of the serum testosterone levels in the offspring male mice, suggesting its exposure may harmfully affect Leydig cell function. We speculate that the decreased testosterone levels in offspring male mice induced by prenatal BPA exposure contribute to the impairments of spermatogenesis. During testosterone synthesis, the acute regulatory protein of steroidogenesis (STAR) plays a crucial role in mediating the transport of cholesterol into the mitochondria, a process essential for testosterone production<sup>33</sup>. Cytochrome P450 cholesterol side-chain cleavage enzyme (CYP11A1) is responsible for the initial and rate-limiting step in steroidogenesis, catalyzing the conversion of cholesterol to pregnenolone, a precursor for various steroid hormones, including testosterone. Pregnenolone is further converted into progesterone or androstenedione by  $3\beta$ -hydroxysteroid dehydrogenase (HSD3B) and cytochrome P450 17 $\alpha$ -hydroxylase/17,20-lyase (CYP17A1). Androstenedione can be catalyzed into testosterone

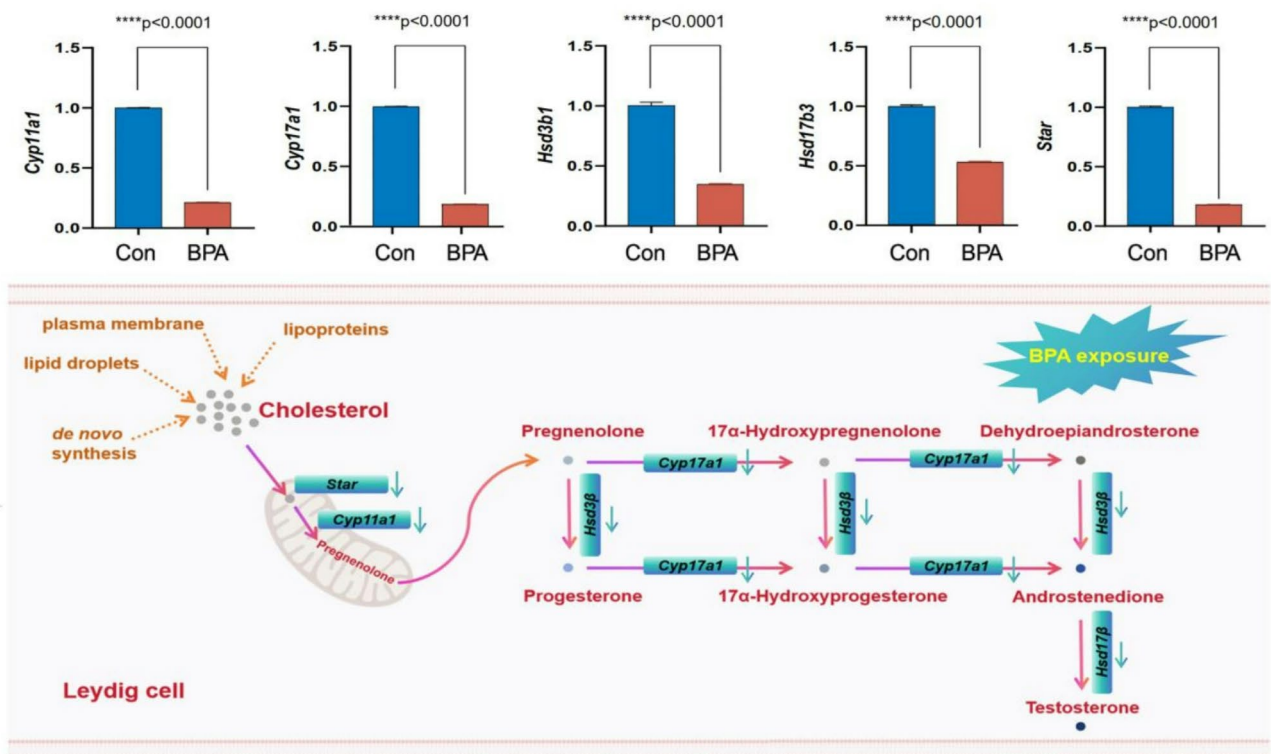


**Fig. 10.** Disturbance of the testosterone synthesis pathway in BPA-exposed Leydig cells. In Leydig cells, androgens are synthesized from cholesterol sourced from the plasma membrane, as well as through de novo synthesis, lipoproteins, and lipid droplets. Protein Star facilitates the transport of cholesterol into the mitochondria, where it is then converted into pregnenolone by Cyp11a1 located in the inner mitochondrial membrane. Pregnenolone is further catalyzed into testosterone through the sequential action of Cyp11a1, Hsd3b, and Hsd17b. The expressions of testosterone synthesis-related genes (*Star*, *Cyp11a1*, *Cyp17a1*, *Hsd3b*, and *Hsd17b*) were statistically down-regulated in BPA-exposed Leydig cells by t-test analysis ( $p < 0.05$ ). The figure was made by using Biorender system ([www.biorender.com](http://www.biorender.com)).

by 17 $\beta$ -hydroxysteroid dehydrogenase (HSD17B)<sup>34–37</sup>. BPA has been showed to impair the expressions of genes associated with testosterone production, specifically Cyp11a1 and Cyp17a1<sup>38</sup>. Administration of BPA at doses of 100 and 200 mg/kg/day to male Sprague-Dawley rats from postnatal day 35 to 56 days leads to a reduced expression of Cyp11a1 and Cyp17a1. The results in hypergonadotropic androgen deficiency in immature Leydig cells and a direct inhibition of 17 $\beta$ -hydroxysteroid dehydrogenase 3 activity<sup>39</sup>. Our findings are consistent with previous research, indicating that prenatal exposure to BPA leads to down-regulation of specific genes in offspring mice. This is not only confirms existing knowledge but also expands our understanding of the potential long-term effects.

Furthermore, we examined the effects of BPA on the proliferation of Leydig cells. The CCK8 proliferation assay revealed significant suppression of Leydig cell proliferation upon exposure to varying BPA concentrations, demonstrating a clear dose-dependent inhibitory effect. Flow cytometry assays further indicated increased apoptosis among Leydig cells exposed to BPA, accompanied by a cell cycle arrest at the G0/G1 phase. Our study further confirmed that this trend was positively correlated with BPA concentrations. Therefore, BPA exposure may be an important factor affecting spermatogenesis in mice. In this study, we found that offspring exposed to BPA during pregnancy also had significantly reduced IVF ability in their sperm as adults. This suggest that avoiding exposure to endocrine disruptors is necessary to ensure reproductive health in offspring. To better understand the effects of BPA exposure on Leydig cells, we also identified differential levels of Leydig cell function and their relationship with BPA exposure. Interestingly, the down-regulation of proteins in Leydig cells by BPA appears to be primarily associated with biological processes such as estrogen response, apoptosis, and centrosome duplication, as suggested by studies on glucocorticoid-induced apoptosis in Leydig cells and the role of NFAT in regulating FasL expression. Xenoestrogen BPA facilitates steroidogenesis in mouse Leydig cells via attenuation of testosterone metabolism. This can cause premature maturation of Leydig cells, characterized by an abnormal intratesticular paracrine milieu and disturbing proper development of germ cells<sup>40</sup>. Our findings indicated that BPA exposure disrupted the protein expressions of the estrogen receptor and the steroid hormone receptor ERR2, aligning with our PCR outcomes for the genes Cyp11a1, Cyp17a1, Hsd3b1, and Hsd3b6. Moreover, the proteins cyclin-H and cyclin-L2 were also downregulated upon BPA exposure, correlating with cell cycle arrest observed in our study. On the other hand, up-regulated Leydig cell proteins were involved in lipid metabolic processes, cellular oxidant detoxification and ROS metabolic process. Bisphenol S(BPS) is a novel

BPA analogue, can induce ROS in immature Leydig cells and directly inhibit the activity of 17 $\beta$ -hydroxysteroid dehydrogenase 3, leading to hypergonadotropic androgen deficiency in male rats<sup>41</sup>. Our work showed that under BPA exposure, the expression of oxidoreductase activity related proteins was up-regulated. These proteins included 24-dehydrocholesterol reductase, acyl-Coenzyme A oxidase 1, aldehyde dehydrogenase 1 family member L2, cytochrome P450 family 1 subfamily b polypeptide 1, cytochrome P450 family 51, cytochrome b5 reductase 1, dehydrogenase/reductase 3, and dehydrogenase/reductase 9. This up-regulation potentially leads to excessive ROS production. Consequently, ROS metabolic process related proteins consisting of microsomal glutathione S-transferase 3, BCL2/adenovirus E1B interacting protein 3, Mpv17 mitochondrial inner membrane protein, and cellular communication network factor 2 were up-regulated and might be used to resist the negative impact of excessive ROS. Pathway analysis revealed that the toll-like receptor signaling pathway was abundant in down-regulated proteins, including S100 calcium binding proteins A8 and A9, as well as estrogen receptor 1. These findings enhance our understanding of the adverse effects of bisphenol A on Leydig cells<sup>42,43</sup>. The proteins identified in this study provide vital information for further examination of the molecular mechanisms of BPA's effects on Leydig cell functions.

Our previous research focused on the effects of BPA exposure on the reproductive potential of male mice. However, little attention has been paid to the effects of prenatal exposure on the reproductive potential of offspring mice. In this study, we found that exposure during pregnancy causes significant damage to interstitial cells in offspring mice compared to damage to spermatogenic epithelial cells. This damage leads to a decrease in the expression levels of androgen metabolism genes, which in turn leads to a decreased serum testosterone levels. These changes further impair the quality of sperm production. There is an elevated proportion of headless and incomplete acrosome sperms, leading to decreased sperm-egg binding ability and disorders in early embryonic development, likely due to oxidative stress and DNA damage during spermatogenesis<sup>44</sup>. Prenatal BPA exposure also disturbed steroidogenesis and arrested the meiotic zygotene-pachytene transition during spermatogenesis. Furthermore, quantitative proteomics of BPA-exposed Leydig cells revealed that differentially expressed proteins were mainly related to steroid hormone receptor activity, centrosome duplication processes, and ROS metabolic processes. In conclusion, differentially expressed proteins mediating the BPA-induced decline in Leydig cells were identified. This study provides additional information for understanding the molecular mechanisms of prenatal BPA exposure and its effects on offspring male reproduction. These findings significantly advance our understanding of how BPA impacts intergenerational male fertility.

Despite these advancements, our current research has not yet thoroughly investigated the roles of signaling pathways and epigenetic modifications in spermatogenesis. Although proteomic analyses have identified certain dysregulated signaling pathways, mechanistic validation—such as through gene knockout models—is still required to establish causal relationships. Future studies should focus on exploring epigenetic mechanisms, including DNA methylation and their potential transgenerational effects, as well as evaluating intervention strategies, such as antioxidant administration, to mitigate ROS-mediated reproductive damage. However, relying solely on mouse models may not fully capture the complexity of human reproductive physiology. To date, large-scale monitoring of BPA levels in pregnant women has not been conducted, and there is a lack of long-term follow-up studies to determine whether their male offspring may develop infertility. To address these limitations and enhance the clinical translational value of our research, we plan to establish correlations between our findings and clinical male infertility. By integrating these research directions, we aim to systematically uncover the regulatory mechanisms of spermatogenesis and provide new theoretical foundations and intervention strategies for the prevention and treatment of male infertility. This comprehensive approach will bridge the gap between animal models and human reproductive health, ultimately contributing to a deeper understanding of the intergenerational effects of environmental exposures such as BPA.

## Conclusions

In general, maternal exposure to BPA during pregnancy can reduce offspring sperm quality primarily by impairing germ cell proliferation and cell cycle, disturbing androgen metabolism, diminished sperm motility. These effects markedly inhibited the sperm-oocyte binding ability and subsequent early embryonic development. This study demonstrates that prenatal BPA exposure impairs offspring sperm quality through multi-faceted mechanisms, including Leydig cell apoptosis, steroidogenic disruption, and meiotic arrest, ultimately leading to subfertility. Therefore, it is necessary to mitigate the risk of reduced offspring fertility caused by BPA exposure during pregnancy. Future studies should focus on elucidating the mechanisms of key molecules involved in the regulation of BPA's effects on male fertility. This research provides crucial evidence that maternal exposure to bisphenol A during pregnancy impairs sperm quality and fertilization potential in male offspring mice, thereby necessitating protective strategies for male reproductive health.

## Data availability

Data is provided within the manuscript or supplementary information files.

Received: 5 December 2024; Accepted: 7 March 2025

Published online: 21 March 2025

## References

1. Dabeer, S. et al. Transgenerational effect of parental obesity and chronic parental bisphenol A exposure on hormonal profile and reproductive organs of preadolescent Wistar rats of F1 generation: A one-generation study. *Hum. Exp. Toxicol.* **39**, 59–76 (2020).
2. Basak, S., Das, M. K. & Duttaroy, A. K. Plastics derived endocrine-disrupting compounds and their effects on early development. *Birth Defects Res.* **112**, 1308–1325 (2020).

3. Lin, M. H., Lee, C. Y., Chuang, Y. S. & Shih, C. L. Exposure to bisphenol A associated with multiple health-related outcomes in humans: An umbrella review of systematic reviews with meta-analyses. *Environ. Res.* **237**, 116900 (2023).
4. Presunto, M., Mariana, M., Lorigo, M. & Cairrao, E. The effects of bisphenol A on human male infertility: A review of current epidemiological studies. *Int. J. Mol. Sci.* **24**, 12417 (2023).
5. Gore, A. C. et al. Executive summary to EDC-2: The endocrine society's second scientific statement on endocrine-Disrupting chemicals. *Endocr. Rev.* **36**, 593–602 (2015).
6. Pagotto, R. et al. Perinatal exposure to bisphenol A disturbs the early differentiation of male germ cells. *Reprod. Toxicol.* **98**, 117–124 (2020).
7. Mondal, S. & Bandyopadhyay, A. Bisphenol A and male murine reproductive system: Finding a link between plasticizer and compromised health. *Toxicol. Sci.* **183**, 241–252 (2021).
8. Owczarek, K., Kudlak, B., Simeonov, V., Mazerska, Z. & Namieśnik, J. Binary mixtures of selected bisphenols in the environment: Their toxicity in relationship to individual constituents. *Molecules* **23**, 3226 (2018).
9. Jurek, A. & Leitner, E. Analytical determination of bisphenol A (BPA) and bisphenol analogues in paper products by LC–MS/MS. *Food Addit. Contam. Part. Chem. Anal. Control Expo Risk Assess.* **35**, 2256–2269 (2018).
10. Gupta, H. & Deshpande, S. B. Bisphenol A decreases the spontaneous contractions of rat uterus in vitro through a nitrenergic mechanism. *J. Basic. Clin. Physiol. Pharmacol.* **29**, 593–598 (2018).
11. Braun, J. M. Early-life exposure to EDCs: Role in childhood obesity and neurodevelopment. *Nat. Rev. Endocrinol.* **13**, 161–173 (2017).
12. Wang, Z. et al. Bisphenol A and pubertal height growth in school-aged children. *J. Expo Sci. Environ. Epidemiol.* **29**, 109–117 (2019).
13. Zulkifli, S., Rahman, A. A., Kadir, S. H. S. A. & Nor, N.S.M. Bisphenol A and its effects on the systemic organs of children. *Eur. J. Pediatr.* **180**, 3111–3127 (2021).
14. Chianese, R. et al. Bisphenol A in reproduction: Epigenetic effects. *Curr. Med. Chem.* **25**, 748–770 (2018).
15. Ryu, D. Y. et al. Abnormal histone replacement following BPA exposure affects spermatogenesis and fertility sequentially. *Environ. Int.* **170**, 107617 (2022).
16. Zhang, T. et al. Melatonin protects prepubertal testis from deleterious effects of bisphenol A or diethylhexyl phthalate by preserving H3K9 methylation. *J. Pineal Res.* **65**, e12497 (2018).
17. Mao, Y. et al. Prenatal BPA exposure disrupts male reproductive functions by interfering with DNA methylation and GDNF expression in the testes of male offspring rats. *Environ. Sci. Pollut. Res. Int.* **30**, 53741–53753 (2023).
18. Varma, S. et al. Fetal exposure to endocrine Disrupting-Bisphenol A (BPA) alters testicular fatty acid metabolism in the adult offspring: Relevance to sperm maturation and quality. *Int. J. Mol. Sci.* **24**, 3769 (2023).
19. Liu, X., Wang, Z. & Liu, F. Chronic exposure of BPA impairs male germ cell proliferation and induces lower sperm quality in male mice. *Chemosphere* **262**, 127880 (2021).
20. Liu, Y. et al. Melatonin improves the ability of spermatozoa to bind with oocytes in the mouse. *Reprod. Fertil. Dev.* **35**, 445–457 (2023).
21. Meistrich, M. L. & Hess, R. A. Assessment of spermatogenesis through staging of seminiferous tubules. *Methods Mol. Biol.* **927**, 299–307 (2013).
22. Peters, A. H., Plug, A. W., van Vugt, M. J. & de Boer, P. A drying-down technique for the spreading of mammalian meiocytes from the male and female germline. *Chromosome Res.* **5**, 66–68 (1997).
23. Rieger, A. M., Nelson, K. L., Konowalchuk, J. D. & Barreda, D. R. Modified Annexin V/propidium iodide apoptosis assay for accurate assessment of cell death. *J. Vis. Exp.* **50**, 2597 (2011).
24. Sunman, B. et al. Prenatal bisphenol A and phthalate exposure are risk factors for male reproductive system development and cord blood sex hormone levels. *Reprod. Toxicol.* **87**, 146–155 (2019).
25. Pallotti, F. et al. Mechanisms of testicular disruption from exposure to bisphenol A and phthalates. *J. Clin. Med.* **9**, 471 (2020).
26. Uchtmann, K. S. et al. Fetal bisphenol A and ethinylestradiol exposure alters male rat urogenital tract morphology at birth: Confirmation of prior low-dose findings in CLARITY-BPA. *Reprod. Toxicol.* **91**, 131–141 (2020).
27. Richter, C. A. et al. In vivo effects of bisphenol A in laboratory rodent studies. *Reprod. Toxicol.* **24**, 199–224 (2007).
28. Cooper, T. G. Looking down on sperm motion: A useful added dimension? *Asian J. Androl.* **16**, 567 (2014).
29. Mahadevaiah, S. K. et al. Recombinational DNA double-strand breaks in mice precede synapsis. *Nat. Genet.* **27**, 271–276 (2001).
30. Qian, B. et al. RNA binding protein RBM46 regulates mitotic-to-meiotic transition in spermatogenesis. *Sci. Adv.* **8**, eabq2945 (2022).
31. Cheng, C. Y. & Mruk, D. D. A local autocrine axis in the testes that regulates spermatogenesis. *Nat. Rev. Endocrinol.* **6**, 380–395 (2010).
32. Zhou, R. et al. The roles and mechanisms of Leydig cells and myoid cells in regulating spermatogenesis. *Cell. Mol. Life Sci.* **76**, 2681–2695 (2019).
33. Stocco, D. M. StAR protein and the regulation of steroid hormone biosynthesis. *Annu. Rev. Physiol.* **63**, 193–213 (2001).
34. Xue, Z. et al. VDR mediated HSD3B1 to regulate lipid metabolism and promoted testosterone synthesis in mouse Leydig cells. *Genes Genomics* **44**, 583–592 (2022).
35. Paradiso, E. et al. Protein kinase B (Akt) Blockade inhibits LH/hCG-mediated 17 $\beta$ -HSD activity; but not 17 $\alpha$ -hydroxylase activity of Cyp17a1 in mouse Leydig cell steroidogenesis. *Cell. Signal.* **111**, 110872 (2023).
36. Rebourcet, D. et al. Ablation of the canonical testosterone production pathway via knockout of the steroidogenic enzyme HSD17B3; reveals a novel mechanism of testicular testosterone production. *FASEB J.* **34**, 10373–10386 (2020).
37. Zirkin, B. R. & Papadopoulos, V. Leydig cells: Formation; function; and regulation. *Biol. Reprod.* **99**, 101–111 (2018).
38. Naciff, J. M. et al. Gene expression changes induced in the testis by transplacental exposure to high and low doses of 17 $\alpha$ -ethynyl estradiol; Genistein; or bisphenol A. *Toxicol. Sci.* **86**, 396–416 (2005).
39. Li, Q. et al. In utero di-(2-ethylhexyl) phthalate-induced testicular dysgenesis syndrome in male newborn rats is rescued by taxifolin through reducing oxidative stress. *Toxicol. Appl. Pharmacol.* **456**, 116262 (2022).
40. Savchuk, I., Söder, O. & Svechnikov, K. Mouse Leydig cells with different androgen production potential are resistant to estrogenic stimuli but responsive to bisphenol A which attenuates testosterone metabolism. *PLoS One.* **8**, e71722 (2013).
41. Pan, P. et al. Bisphenol S stimulates Leydig cell proliferation but inhibits differentiation in pubertal male rats through multiple mechanisms. *Environ. Toxicol.* **38**, 2361–2376 (2023).
42. Karunarathne, W. A. H. M. et al. A potential Toll-like receptor 4/myeloid differentiation factor 2 complex agonist. *Environ. Pollut.* **278**, 116829 (2021).
43. Liu, Z. et al. Glutamine attenuates bisphenol A-induced intestinal inflammation by regulating gut microbiota and TLR4-p38/MAPK-NF- $\kappa$ B pathway in piglets. *Ecotoxicol. Environ. Saf.* **270**, 115836 (2024).
44. Rotimi, D. E. & Singh, S. K. Implications of lifestyle factors on male reproductive health. *JBRA Assist. Reprod.* **28**, 320–330 (2024).

## Acknowledgements

We sincerely thank Professor Lan Ye from the National Key Laboratory of Reproductive Medicine and Offspring Health at Nanjing Medical University (Nanjing) for her technical guidance and assistance in chromosome spreading technology, and also sincerely thank Professor Wantao Ying from the National Protein Science Center



(Beijing) for his technical guidance and assistance in proteomics technology. This work was supported by grants from Shandong Provincial Natural Science Foundation, China (ZR2022MH020), and Fundamental Research Projects of Science & Technology Innovation and Development Plan in Yantai City, China (2022JCYJ039).

### Author contributions

W.Z. and J.L. have made equal contributions to this manuscript and are co-first authors. Conceptualization, X. L., Y. W., and J. L.; methodology, W. Z., Y. W., J. L., W.W., P. Z., Y. W., J. W., J. L.; software, X. L., Y. W., J.W. and J. L.; validation, W. Z., Y. W., J. L., P. Z., Y. W., J. W., J. L.; formal analysis, W. Z., Y. W., J. L., P. Z., Y. W., J. W., J. L.; investigation, X. L., Y. W., and J. L.; resources, X. L., Y. W., and J. L.; data curation, X. L., Y. W., and J. L.; writing—original draft preparation, W. Z., Y. W., J. W., P.Z., Z.S., W.W.,J.L., D.S., Y. W., J. L., and X. L.; writing—review and editing, X. L., Y. W., and J. L.; visualization, X. L., Y. W., and J. L.; supervision, X. L., Y. W., and J. L.; project administration, X. L., Y. W., and J. L.; funding acquisition, X. L., Y. W., and J. L. All authors have read and agreed to the published version of the manuscript.

### Declarations

### Competing interests

The authors declare no competing interests.

### Additional information

**Supplementary Information** The online version contains supplementary material available at <https://doi.org/10.1038/s41598-025-93538-9>.

**Correspondence** and requests for materials should be addressed to Y.W. or X.L.

**Reprints and permissions information** is available at [www.nature.com/reprints](http://www.nature.com/reprints).

**Publisher's note** Springer Nature remains neutral with regard to jurisdictional claims in published maps and institutional affiliations.

**Open Access** This article is licensed under a Creative Commons Attribution-NonCommercial-NoDerivatives 4.0 International License, which permits any non-commercial use, sharing, distribution and reproduction in any medium or format, as long as you give appropriate credit to the original author(s) and the source, provide a link to the Creative Commons licence, and indicate if you modified the licensed material. You do not have permission under this licence to share adapted material derived from this article or parts of it. The images or other third party material in this article are included in the article's Creative Commons licence, unless indicated otherwise in a credit line to the material. If material is not included in the article's Creative Commons licence and your intended use is not permitted by statutory regulation or exceeds the permitted use, you will need to obtain permission directly from the copyright holder. To view a copy of this licence, visit <http://creativecommons.org/licenses/by-nc-nd/4.0/>.

© The Author(s) 2025